Electronic Supplementary Material (ESI) for Journal of Materials Chemistry A.

Supporting Information

Lithium–Sulfur Cells with a Sulfide Solid Electrolyte / Polysulfide Cathode Interface

Yin-Ju Yen[a] and Sheng-Heng Chung[a,b,*]

[a] Department of Materials Science and Engineering, National Cheng Kung University, No. 1, University Road, Tainan City 70101

[b] Hierarchical Green-Energy Materials Research Center, National Cheng Kung University, No. 1, University Road, Tainan City 70101

*Sheng-Heng Chung: SHChung@gs.ncku.edu.tw

Supporting Figures

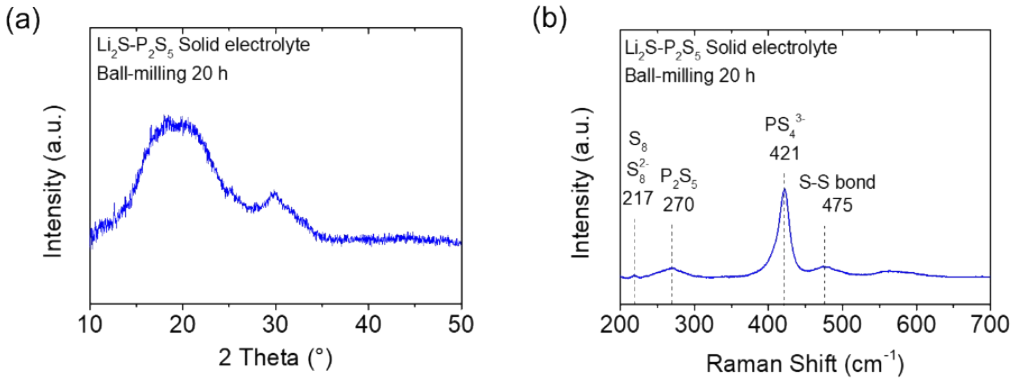

Fig. S1. Crystalline structure and chemical composition of the ball-milled sulfide powder: (a) XRD pattern and (b) Raman spectrum.

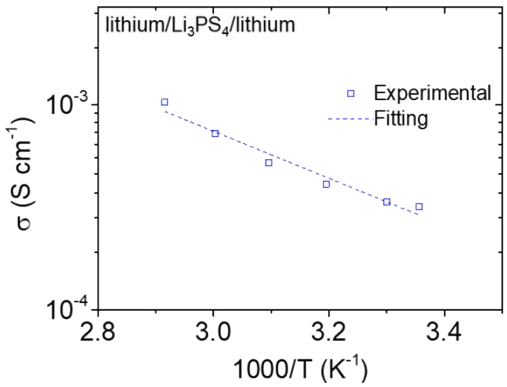

Fig. S2. Lithium/Li_3PS_4/lithium symmetric cell analysis: ionic conductivity of the synthesized Li_3PS_4 solid electrolyte from 25 ℃ to 70 ℃ based on the Arrhenius plot.

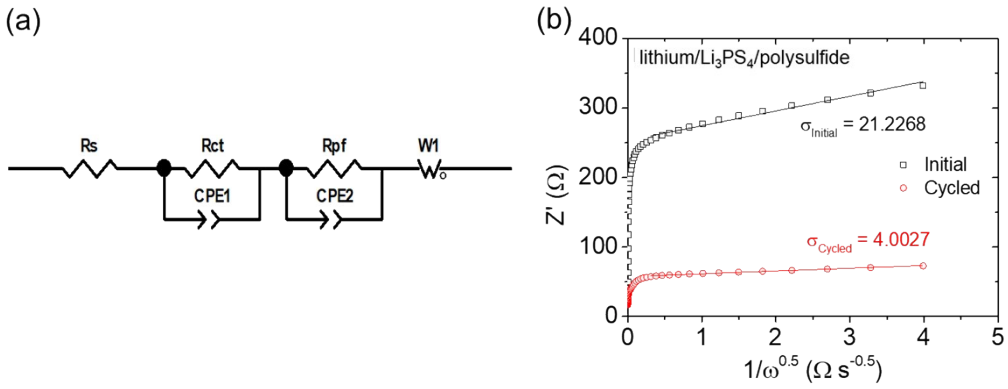

Fig. S3. Electrochemical impedance analysis of a lithium/Li_3PS_4/polysulfide cell: (a) the equivalent Randles circuit of the Nyquist plots before and after cycling and (b) the Warburg factor (σ) determined from the fitting results of the electrochemical impedance analysis based on the Arrhenius equation.

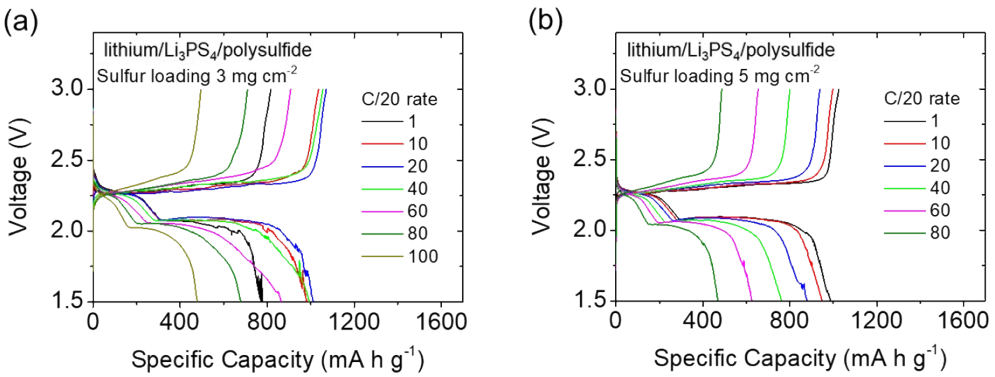

Fig. S4. Charge/discharge curves of the cyclability test of a lithium/Li_3PS_4/polysulfide cell at a C/20 rate with sulfur loadings of (a) 3 mg cm^{-2} and (b) 5 mg cm^{-2}.

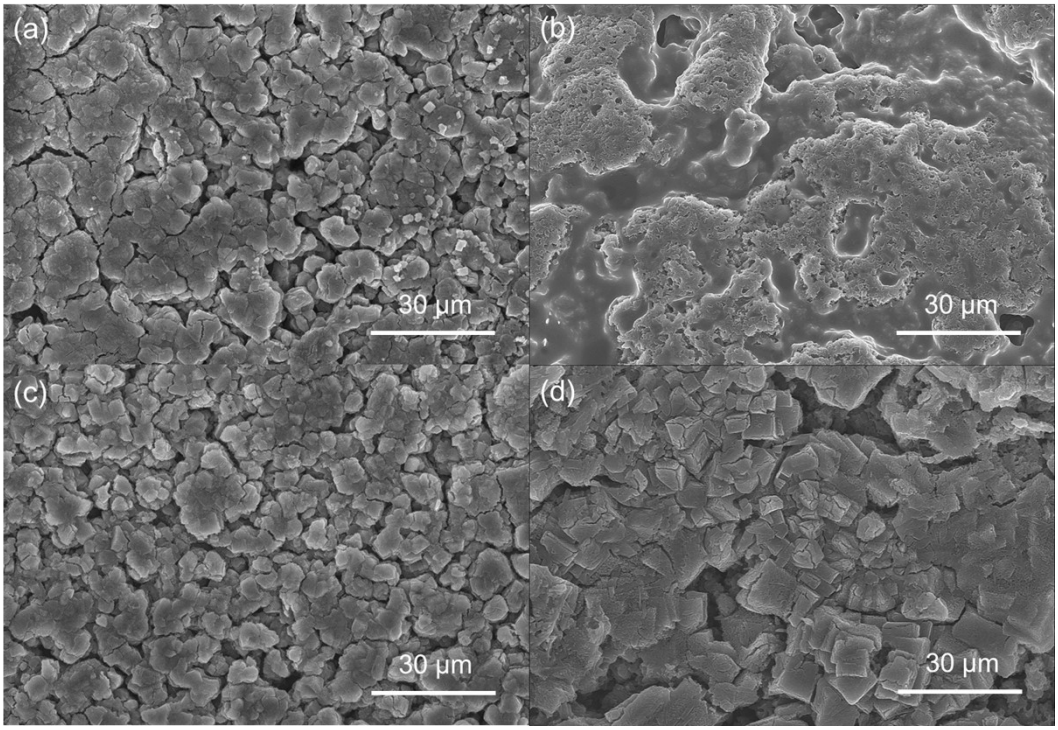

Fig. S5. SEM images of the Li_3PS_4 solid electrolyte on the cathode side surface of (a) fresh and (b) cycled electrolytes, and on the anode side of (c) fresh and (d) cycled electrolytes.

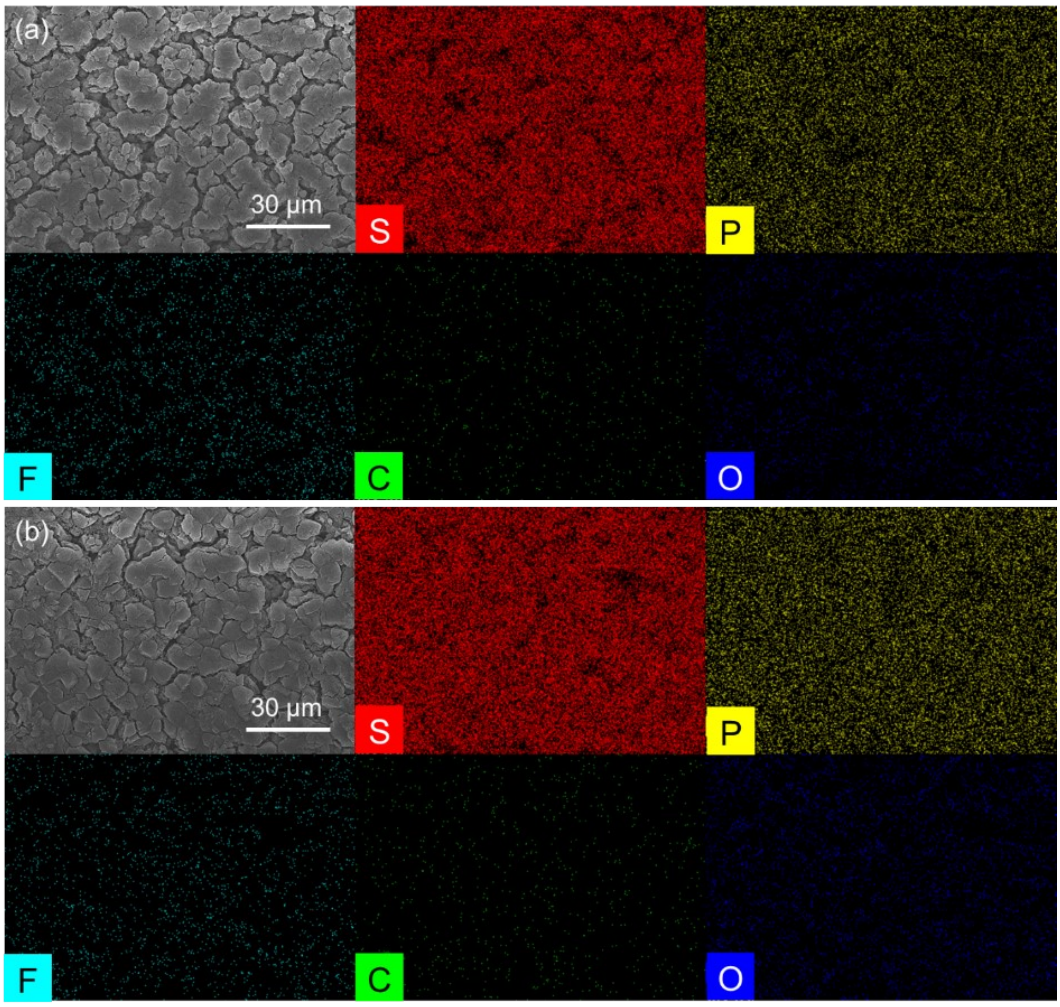

Fig. S6. SEM/EDS results of the fresh Li_3PS_4 solid electrolyte: (a) on the cathode side surface and (b) on the anode side surface.

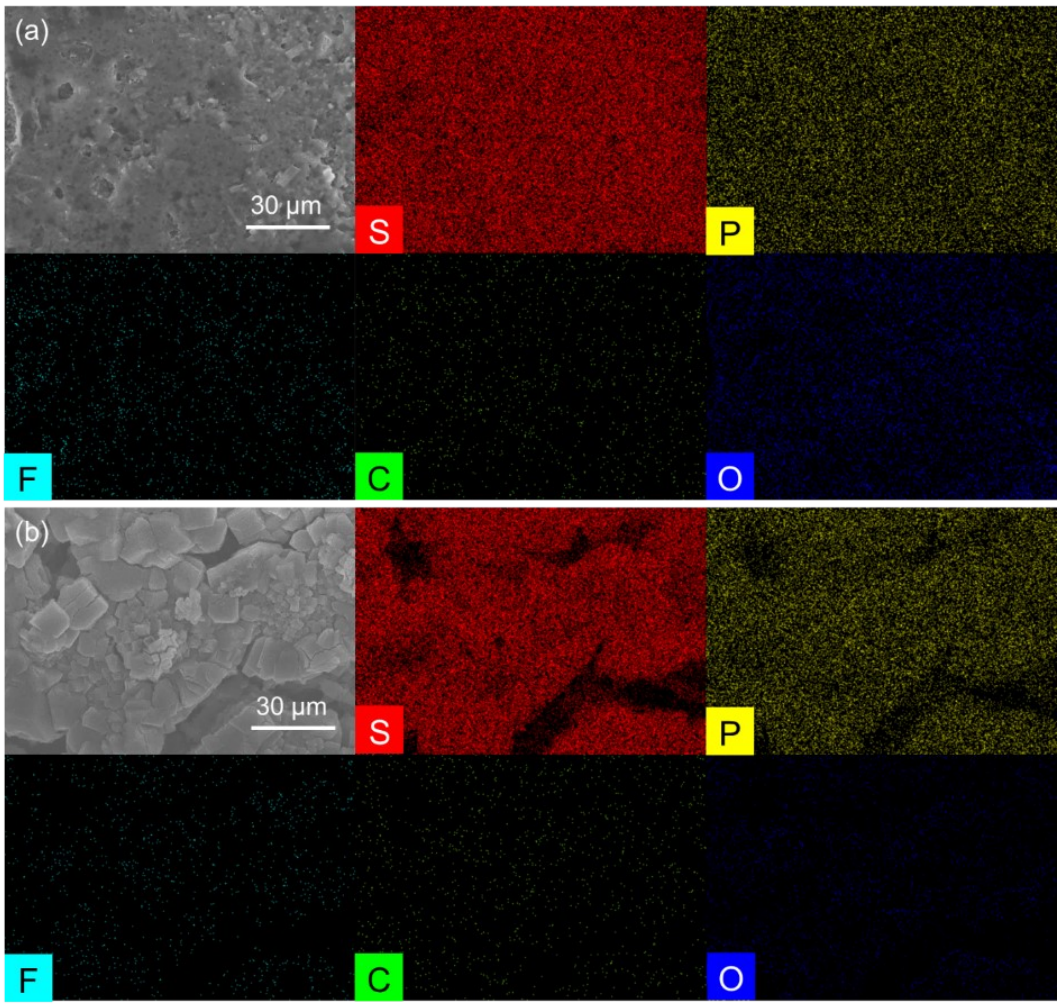

Fig. S7. SEM/EDS results of the cycled Li_3PS_4 solid electrolyte: (a) on the cathode side surface and (b) the anode side surface.

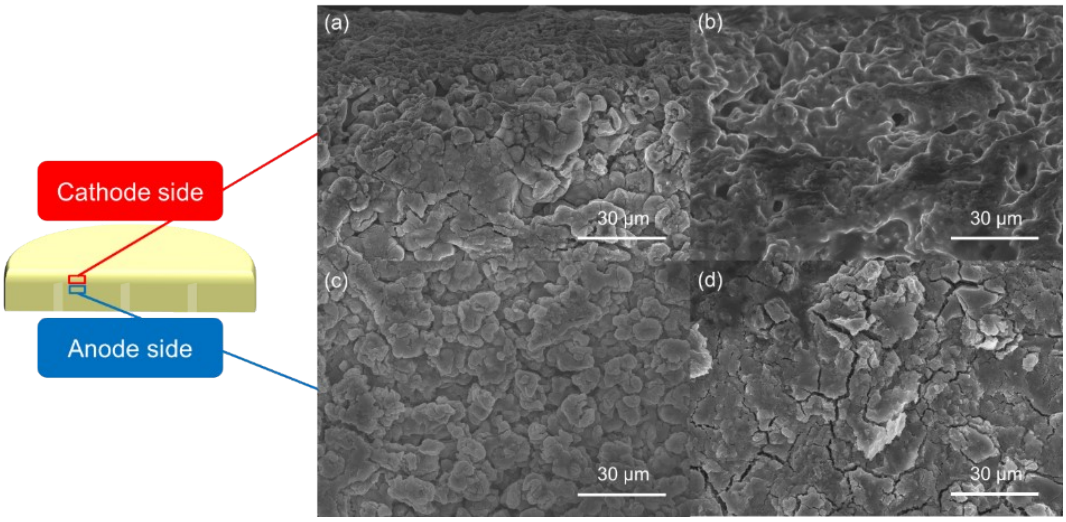

Fig. S8. SEM images of the cross section of (a) and (c) the fresh Li_3PS_4 solid electrolyte, and (b) and (d) the cycled Li_3PS_4 solid electrolyte. The microstructures of (a) and (b) are at the spot nearest to the cathode side, and (c) and (d) are at approximately 90 μm in depth at the cathode side.

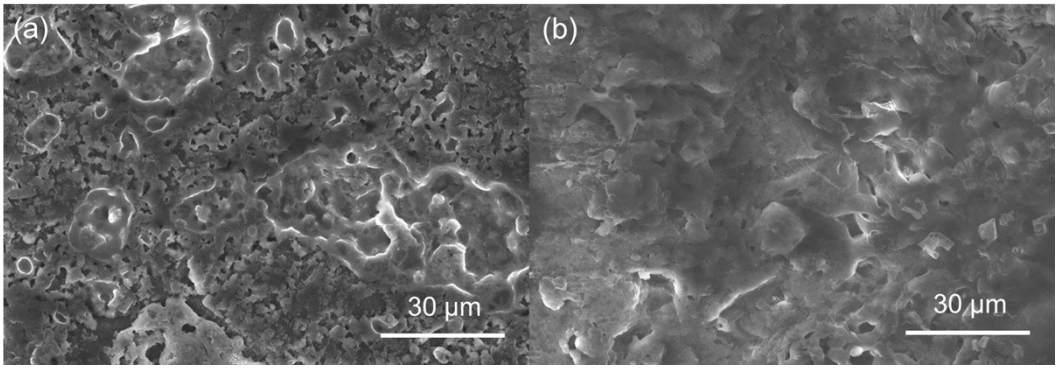

Fig. S9. SEM images of (a) fresh lithium anode and (b) cycled lithium anode.

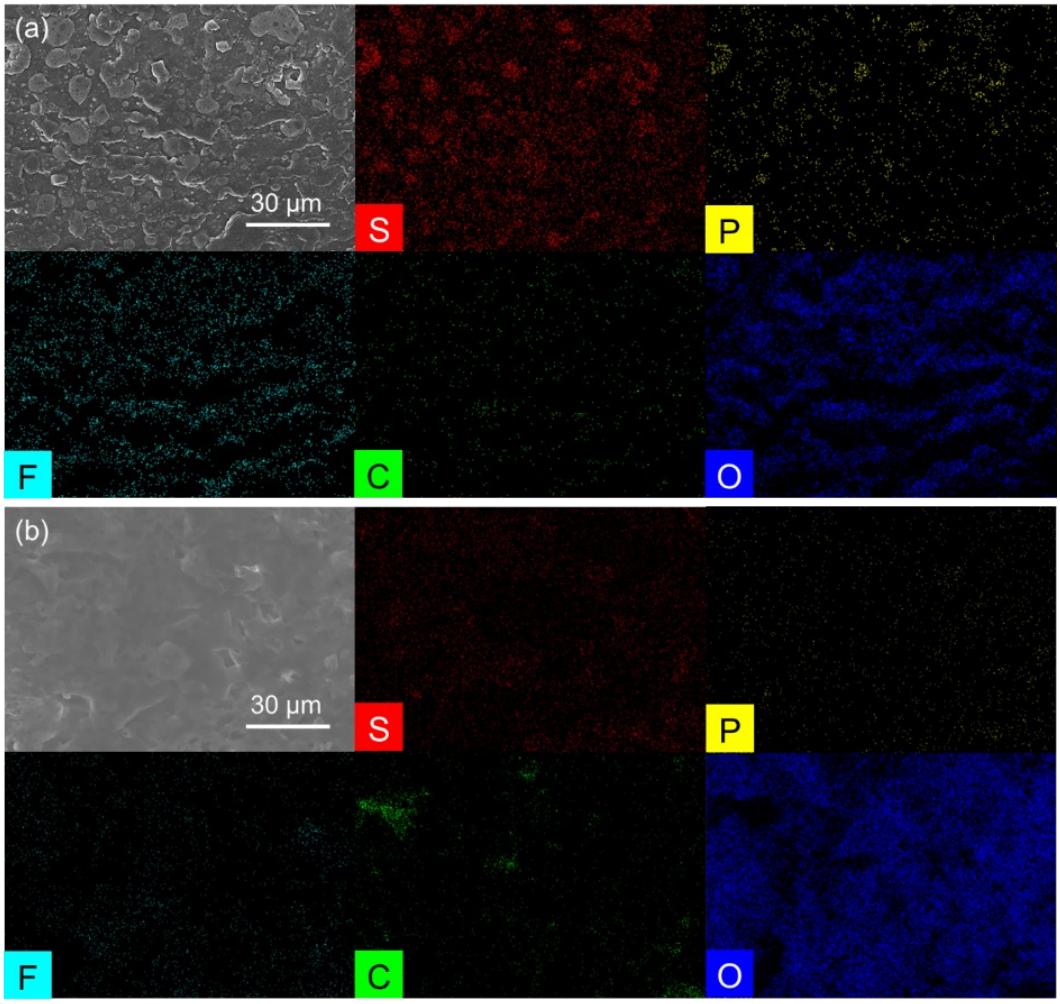

Fig. S10. SEM/EDS results of (a) fresh lithium anode and (b) cycled lithium anode.

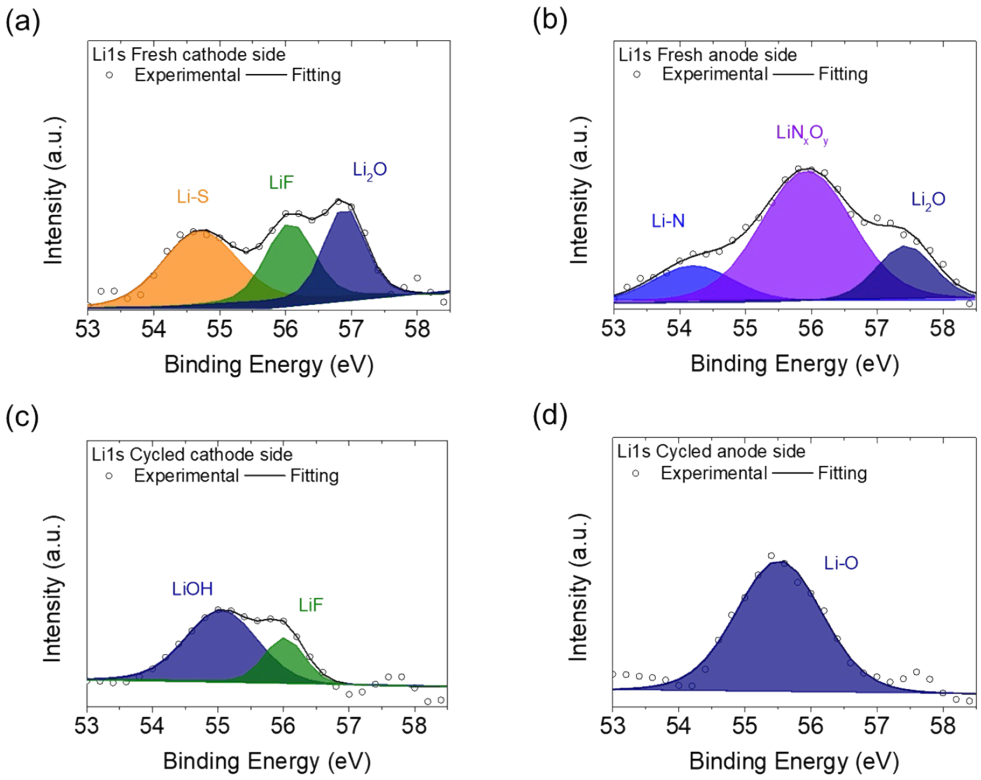

Fig. S11. XPS Li1s spectra of the Li_3PS_4 solid electrolyte: (a) on the cathode side and (b) on the anode side of the fresh electrolyte, and (c) on the cathode side and (d) on the anode side of the cycled electrolyte.

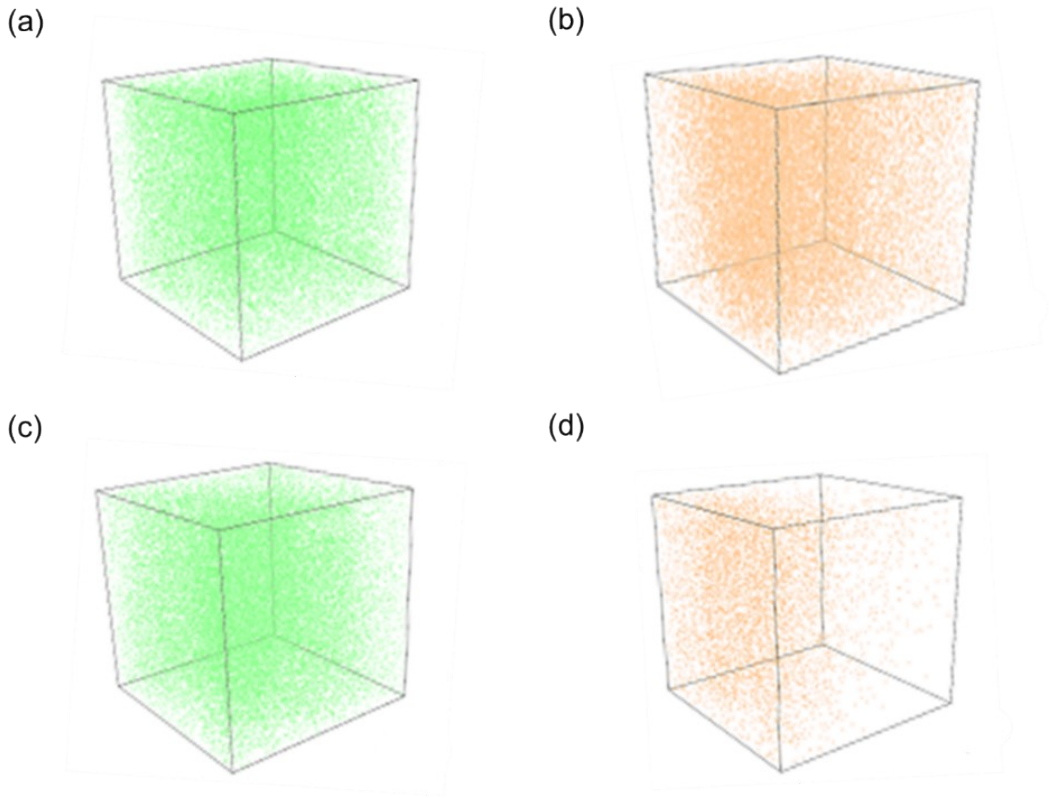

Fig. S12. 3D visualization of LiP^- detected in the Li_3PS_4 solid electrolyte at an inspection depth of 300 nm: (a) on the cathode side of the fresh electrolyte, (b) on the anode side of the fresh electrolyte, (c) on the cathode side of the cycled electrolyte, and (d) on the anode side of the cycled electrolyte.

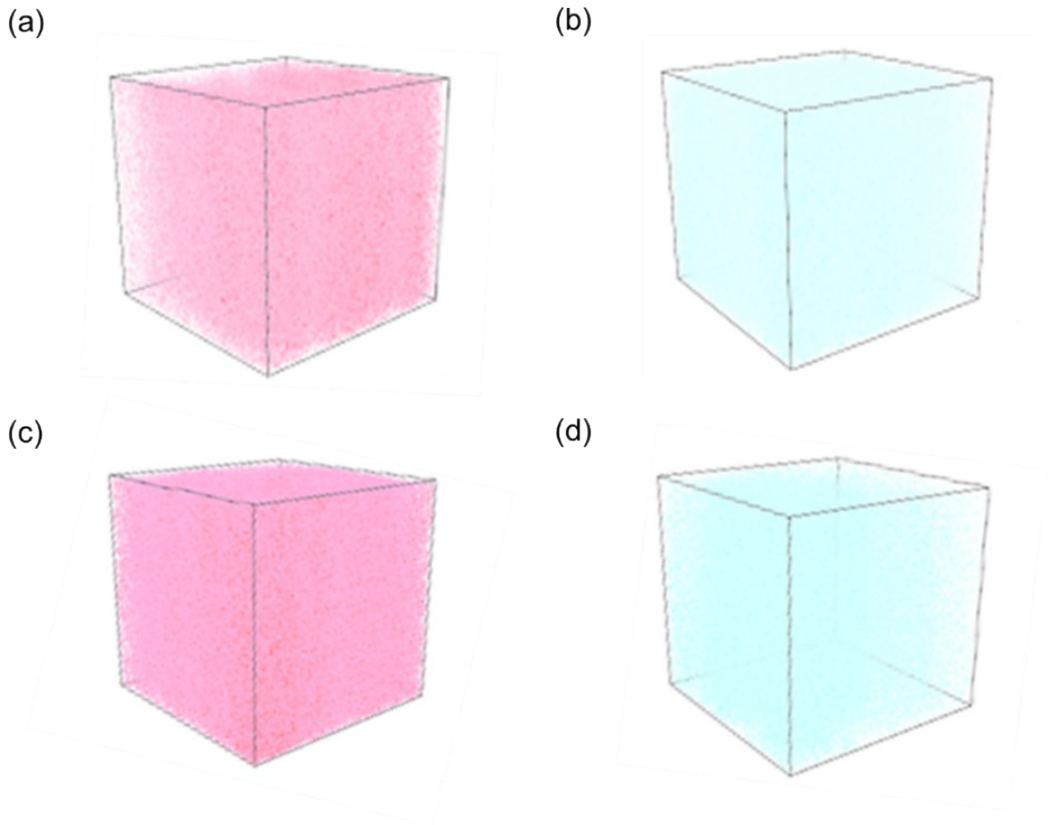

Fig. S13. 3D visualization of PO^- detected in the Li_3PS_4 solid electrolyte with an inspection depth of 300 nm: (a) on the cathode side of the fresh electrolyte, (b) on the anode side of the fresh electrolyte, (c) on the cathode side of the cycled electrolyte, and (d) on the anode side of the cycled electrolyte.

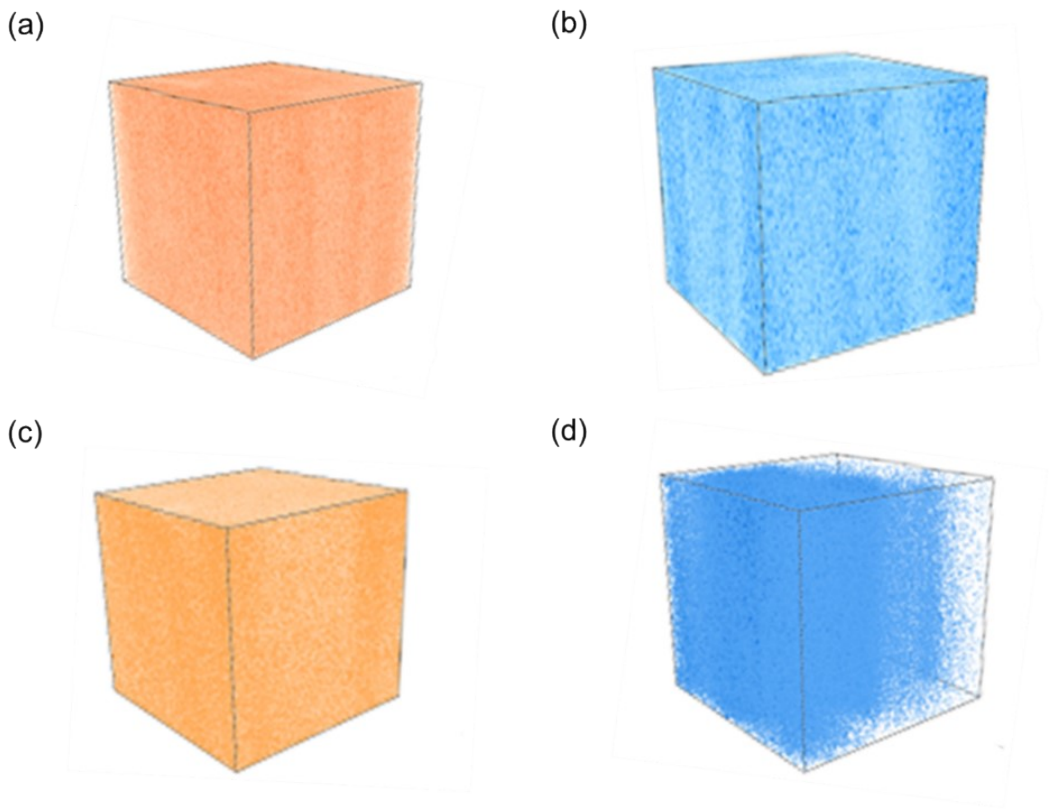

Fig. S14. 3D visualization of S_2O^- detected in the Li_3PS_4 solid electrolyte with an inspection depth of 300 nm: (a) on the cathode side of the fresh electrolyte, (b) on the anode side of the fresh electrolyte, (c) on the cathode side of the cycled electrolyte, and (d) on the anode side of the cycled electrolyte.

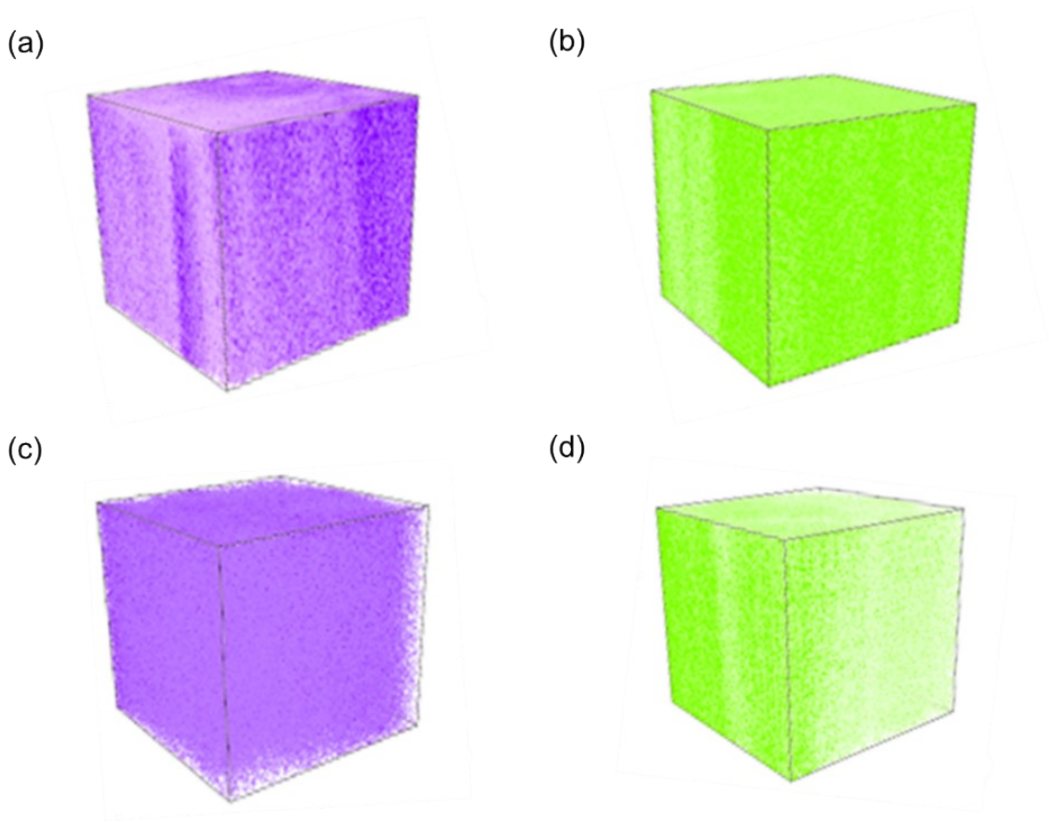

Fig. S15. 3D visualization of PS^- detected in the Li_3PS_4 solid electrolyte with an inspection depth of 300 nm: (a) on the cathode side of the fresh electrolyte, (b) on the anode side of the fresh electrolyte, (c) on the cathode side of the cycled electrolyte, and (d) on the anode side of the cycled electrolyte.